Nuclear Materials and Energy 17 (2018) 15–23

Contents lists available at ScienceDirect

Nuclear Materials and Energy

journal homepage: www.elsevier.com/locate/nme

The design and thermo-structural analysis of target assembly for high intensity neutron source

E. Wakai[a,*], K. Watanabe[b], H. Kondo[c], F. Groeschel[d]

[a] Japan Atomic Energy Agency, Tokai-mura, 319-1195, Japan
[b] Research Organization for Information Science and Technology, Kobe 650-0047 Japan
[c] National Institutes for Quantum and Radiological Science and Technology, Naka 311-0193 Japan
[d] Karlsruhe Institute of Technology, 76131 Karlsruhe, Germany

ARTICLE INFO

Keywords:
High intensity neutron source
Target assembly
Thermo-structural analysis
Li target
IFMIF
F82H

ABSTRACT

The engineering design of an integrated target assembly of IFMIF lithium target was performed in IFMIF/EVEDA project for a high intensity neutron source. In the evaluation of the design, a thermos-structural analysis of was evaluated by ABAQUS code, and the modeling region was a part of the target assembly which was from the inlet nozzle to the outlet pipe. The material of the target assembly including the back plate was F82H steel. In the thermal-structural analysis, the normal operations and start/stop or abnormal operations were evaluated at 250 or 300 °C operation of Li flow in inlet pipe. The result showed that the temperature of the target assembly was evaluated to be still lower than the Li boiling point of 344 °C under a vacuum pressure of 10^{-3} Pa. In a temperature constant operation, the calculated stresses and displacements were small enough for thermal soundness of the target assembly in steady states. In a transient cooling process from 300 °C to 20 °C through 250 °C, the maximum Mises stress was found to be 372 MPa, which was lower than the yield stress at 300 °C.

1. Introduction

The main function of the International Fusion Materials Irradiation Facility (IFMIF) or the other neutron source facilities is to generate the high intense neutrons by injecting the deuteron or proton beams accelerated to high energy onto the target material such as liquid target of Li [1-4], Hg [5–7] Pb-Bi [8,9] and solid target [9–12]. The highest beam power in them is 10 MW of the IFMIF. The engineering validation and design activities (EVEDA) for IFMIF were performed to start from 2007 in a jointed program between the EU and Japan as a Broader Approach (BA) for fusion demo reactor. Some validation test and engineering design for lithium target facility of IFMIF were completed [13–28].

The objective of IFMIF is to generate high intensity neutrons, which are similar to fusion neutrons with 14 MeV, by injecting the deuteron beams accelerated to high energy onto the 260 mm wide and 25 mm thick free-surface lithium flow. Guiding the liquid lithium along the concave back plate at a speed of 15 m/s is required to increase the pressure in the lithium flow by centrifugal force, to avoid boiling by the heat input of the deuteron beams, and to remove heat by the lithium flow circulation [2,29]. This enables the target geometry to be maintained at the time of heat input, which is unexpected for solid target, and realizes the steady-state neutron source. IFMIF is composed of lithium target facility, accelerator facility, test facility with high flux module [14,30] and the other modules, and conventional facility.

In IFMIF operation after EVEDA, intense neutrons are emitted inside the Li flow through a thin back plate attached to the target assembly. Since the back plate is operating under a severe neutron irradiation of 50 dpa/year and a maximum nuclear heating rate of 25 W/cm^3, thermo-structural design is one of critical issues in a target design. The back plate is replaced in annual maintenance after every 11 months operation because of neutron irradiation damage. Two design options of the target assembly for the back plate replacement are under investigation. The first option is an “Integrated type” target assembly where the Li flow channel includes an integral back plate. This option requires replacement of the entire target assembly prior to life time of a portion of it. The second option is a target assembly with replaceable bayonet-type back plate. In this option, only the back plate will be replaced [21,22]. The Guiding the lithium flow along the concave back plate in target assembly at a speed of 15 m/s at 250 °C is required to increase the pressure in the lithium flow by centrifugal force, to avoid boiling by the heat input 10 MW by the 40 MeV deuteron two beams with 250 mA in total, and to remove heat by the lithium flow circulation. In this study, the thermos-structural analysis and the design of an integrated target assembly (TA) of IFMIF lithium target was evaluated.

* Corresponding author.
E-mail address: wakai.eiichi@jaea.go.jp (E. Wakai).

https://doi.org/10.1016/j.nme.2018.07.005
Received 15 December 2017; Received in revised form 27 June 2018; Accepted 11 July 2018

Table 1
Main specification of Li flowing target in IFMIF. Temperature will be increased to 350 °C inside lithium flow by the beam injection. The surface temperature will be elevated up to 280 °C. The margin of boiling temperature at the surface is about 40 °C.

Item	Condition
Heating power	10 MW
Vacuum	$10^{-3} \sim 10^{-2}$ Pa
Li temperature in inlet pipe	250 °C
Flow velocity	15 m/s (max. 16 m/s)
Li flowing thickness and width	0.025 m, 0.26 m
Li thickness variation	$\leqq \pm$ 1 mm
Li amount	9 m^3 (4.5 tons)
Li flow rate	130 l/s

Some of engineering design of lithium target facility of IFMIF were presented by some studies [2–4,13]. The main specification of lithium target facility of IFMIF engineering design is shown in Table 1.

2. System diagram of target assembly of lithium target facility of IFMIF

The system diagram of the lithium target facility was given in Fig. 1. The facility is composed of main lithium loop, lithium target system and target assembly, lithium flow measurement system and diagnostics, target test cell, beam duct, electro-magnetic pump system, impurity monitoring loop, impurity control system (lithium purification loop), quench tank and drain tank system, heat removal system, and remote handling systems.

In the main lithium loop and target assembly, the main Li loop circulates liquid Li through the TA by the main electro-magnetic pump (EMP). The TA with the Li inlet pipe with an outer diameter of 165.2 mm (in JIS, 6B, Sch.40), a part of the Li outlet channel and parts of the beam ducts are in the TC. Temperature of the BP, thickness of which is the thinnest among Li components and most severely irradiated by neutron and gamma ray, is monitored. There is no vacuum port in TC. Beam duct vacuum pressure is maintained by vacuum pumps through vacuum ports both outside of TC. Downstream end of the Li outlet channel is below the Li level in the QT by 0.2 m to suppress Li splash by confinement by duct and Li boiling by the head pressure. Also downstream end of the bypass is below the Li level to avoid cavitation under vacuum condition of QT with reflecting experiences at the EVEDA Lithium Test Loop (ELTL) operation. Temperature and Li level of QT are monitored. A Li overflow line is near the top of QT. Height difference between the overflow and the reference Li level in operation is about 0.2 m corresponding to Li volume beyond the reference level. Vacuum of the QT is maintained at 10^{-3} Pa or less through the surge tank (ST). Also Ar is supplied or evacuated through the ST. There is a gate valve under QT, which is closed at each TA replacement to limit volume exposed atmosphere containing air (O and N). All valves for Li components are opened and closed remotely by pressurized Ar gas, since no worker is accessible to the areas in beam operation when radiation is too high for workers and the areas are filled with Ar gas. Outer diameter of pipes between the QT and the main EMP is 267.4 mm (10B, Sch.20S) for smaller pressure drop to avoid cavitation at the inlet of the EMP located at the lowest among operating Li components, 6.5 m below the Li level in QT. Branch lines to/from the Impurity Reduction System (IRS) are connected to this section. Pressure in this section is low in comparison with the other part of the main Li loop. This condition eases design pressure of the ICS. Li flow rate at the exit of the EMP is finely controlled by feedback with a flow rate measured at the electro-magnetic flow meter (EMFM). Temperature of the EMP coil is monitored for a feedback control on a start of blower for cooling. Outer diameter of pipes downstream the EMP is 216.3 mm (8B,

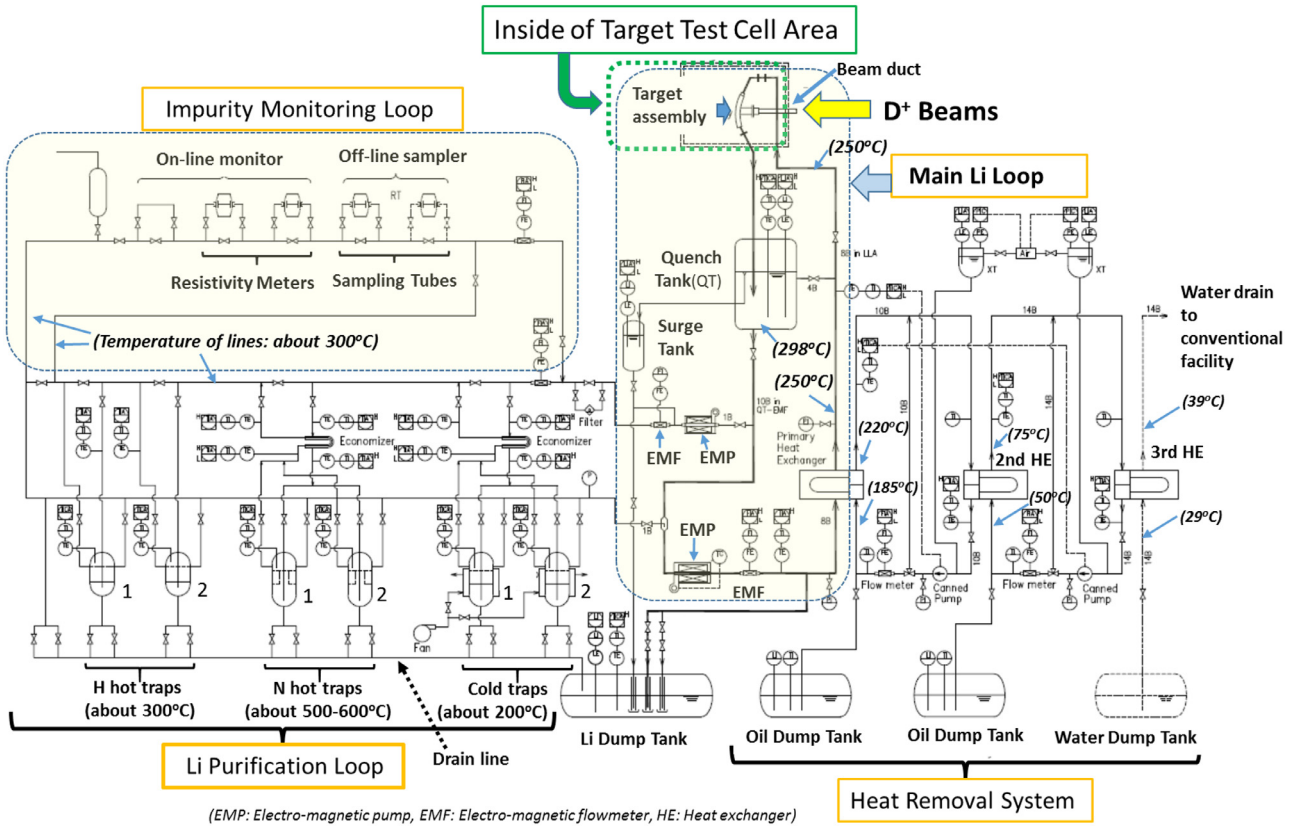

Fig. 1. System diagram of lithium target facility of IFMIF. *(FE: Flow element, FI: Flow indicator, FM: Flow meter, LE: Level element, LI: Level indicator, PE: Pressure element, PI: Pressure indicator, TC: Temperature controller, TE: Temperature element, TI: Temperature indicator, TIC: Temperature indicator controller, XT: Expansion tank).*

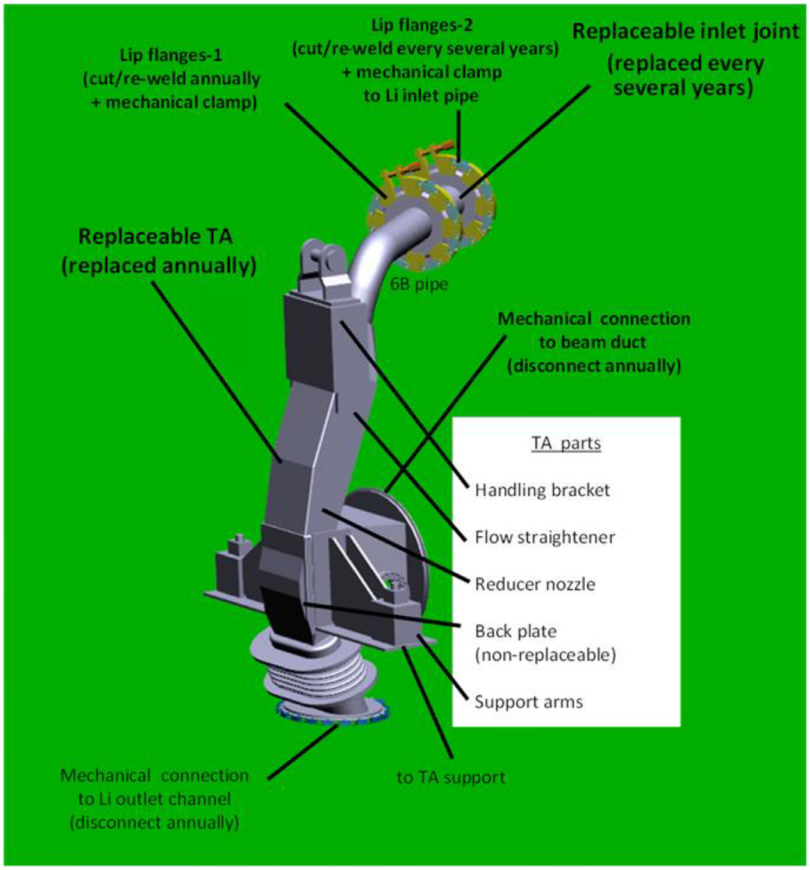

Fig. 2. Target assembly of lithium target facility.

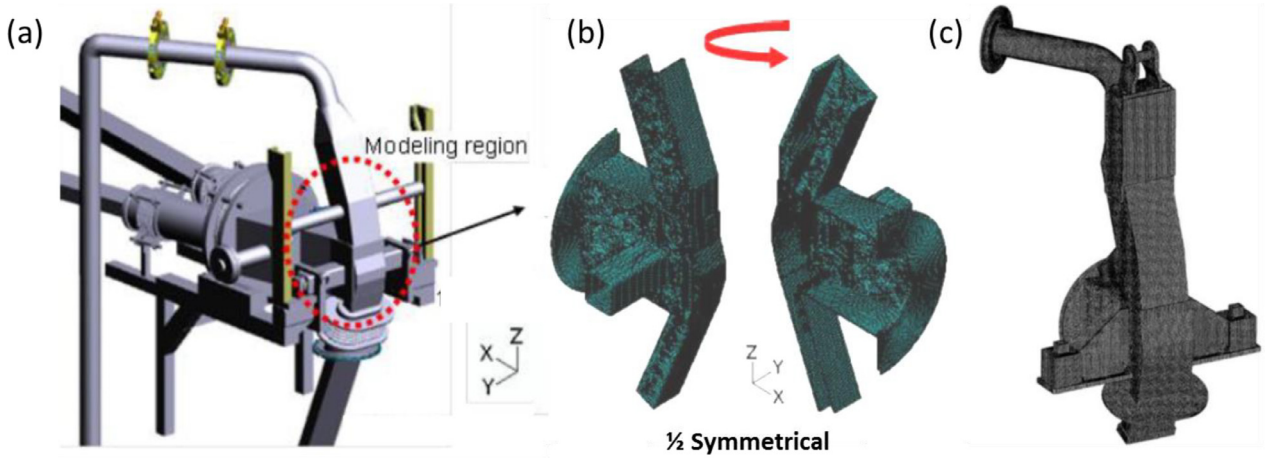

Fig. 3. (a) CATIA CAD model, (b) and (c) ABAQUS mesh model of target assembly.

Sch.20S) in the LLA, but 165.2 mm (6B, Sche.40) in the TC to reduce neutron and gamma ray through the wall penetration. Outer diameter of pipes of the bypass line is 114.3 mm (4B, Sch.20S), since the line is used for rather small flow rate up to 32.5 L/s (equivalent to 5 m/s at the TA nozzle exit) in normal operation. The EMFM is calibrated with monitoring Li level in the QT. For this purpose, the drain line was changed to downstream of the EMFM. The primary heat exchanger (HX1) transfers the heat up 10 MW from liquid Li on the shell side to organic oil ThermS-900® on the tube side. Even while a hotter fluid is on tube side in usual designs of heat exchangers, the liquid is in on the shell side in IFMIF LF design to reduce risk of tube plugging of Li which freezing point is 181 °C far higher than those of oils. In normal operation, pressure of Li in the shell side of HX1 is 196–211 kPa (assuming proportional to square of flow rate, i.e. $(15/16)^2$ times) and pressure of the oil ThermS-900 is 166–180KPa. In case of tube rapture in HX1, leakage is in the direction from the Li to the oil. Pressure of Li at inlet and outlet of the HX1 is monitored by pressure gauges with strain-gauges and membranes inside, whose type is the same as that fabricated for use at the ELTL. A remarkable change in absolute pressure or pressure difference between the two gauges tells malfunctions such as tube/shell rupture or partial plugging, respectively. Temperature of Li at inlet and outlet of the HX1 is monitored. Temperature of Li in the main Li Loop is controlled by feedback with the Li temperature measured at outlet of the HX1 typically. Li flow velocity in the shell side of the HX1 is very low, 0.2 m/s at reference flow rate of 97.5 L/s. Note that heaters and thermo-couples are equipped on not only the outlet of HX1

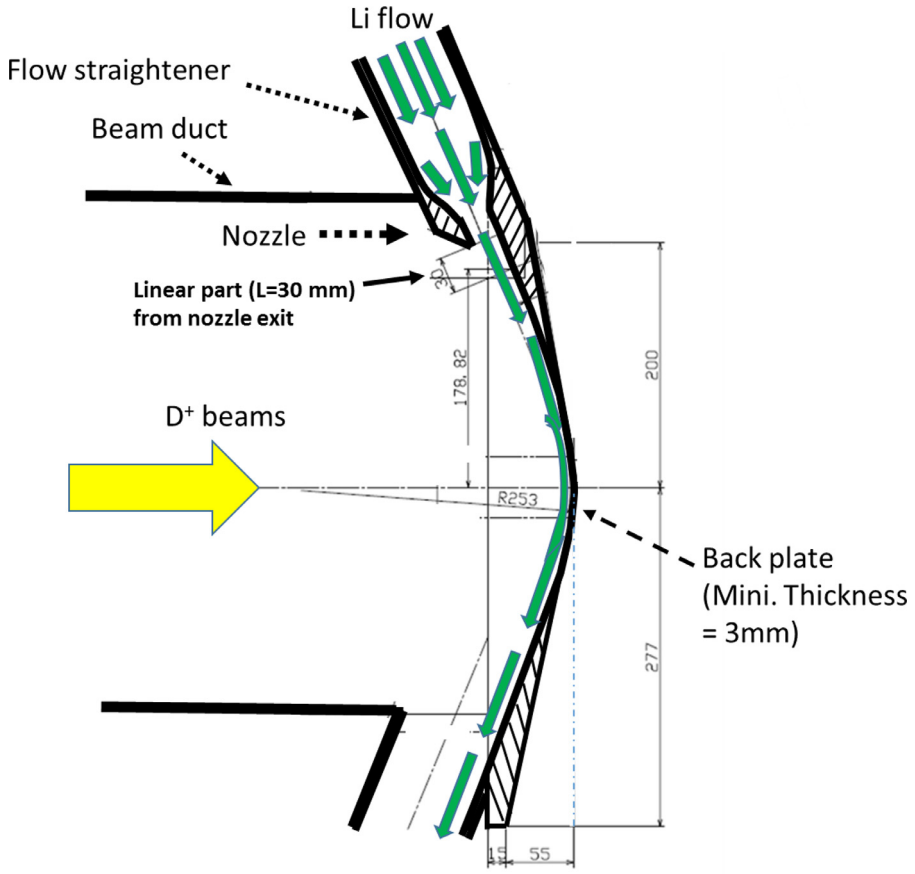

Fig. 4. Schematic image of lithium flow in the back plate of integrated target assembly.

but also everywhere of the main loop except for small area around the BP and vacuum vessel part of TA not contacting to liquid Li. Rapid decrease of Li temperature is achieved by not only no-current in the heater but also increase of the oil flow rate in the secondary loop. There are two drain lines between the main Li loop and the Li dump tank (DT) for redundancy corresponding to malfunctions of gate valves at opening. Furthermore, each drain line has two gate valves corresponding to malfunctions at closing. Temperature of Li in the DT is monitored and controlled. This information is used mainly at Li melting. Also Li level of the Li DT is monitored. This information is used mainly at Li drain and Li charge after Li melting. Pressurized Ar gas is supplied to the Li DT at the Li charge. The Li DT is under vacuum condition in operation, but filled with Ar gas in maintenance.

3. Model of target assembly of IFMIF and the thermo-structure analysis

The thermo-structural analysis for the designed integrated target assembly was performed by ABAQUS code version 6.9. The modeling region was a part of the target assembly as shown in Figs. 2–4 which were from the inlet nozzle to the outlet pipe. The calculations were performed for a half section of the target assembly because of symmetry to *X-Z* plane. *X* axis is the vertical direction of *YZ* plane which is basically the intermediate of two beam directions, *Y* axis is the horizontal direction, and *Z* axis is the perpendicular direction. The Hexa meshes were only used in this model. The material of the target assembly including the back plate was a reduced-activation ferritic/martensitic steel F82H (the main chemical composition: Fe-8Cr-2W-0.1C–0.04Ta) in the calculation model. This calculation simulated pre-heating operation of the IFMIF, so there was no liquid lithium and nuclear heating. In this calculation, some thermal boundary conditions were set to estimate a soundness of the target assembly. The beam chamber and the support arms have radiation surfaces and are not equipped with heaters. The outer surfaces of the lithium flow channel were covered with the heaters, except for the top of the BP. The heater was simulated to load heat flux as input data. Adiabatic boundary condition was adopted to the surfaces with the heaters except for the outer surfaces of the back plate. It was considered that heat was transferred from the BP to the High Flux Test Module (HFTM). Those heat transfer coefficients were calculated. The surface temperature of the HFTM was assumed 50 °C for conservative estimation at heat transfer. On the lithium flow channel i.e. inner surface of the back plate, the radiation to the inside space of the body was considered, and the contact heat transfer was set on the flange.

(1) Calculation model

The thermal and structural calculations by ABAQUS code version 6.9 were done to estimate for strength to the thermal stress of the integrated target assembly. The calculation model was the same as one for the thermal analysis as shown in Figs. 3 and 4, and the thermal boundary condition is shown in Fig. 5.

(2) Calculation conditions

The calculations in this section were classified into two groups as follows. The first group calculations simulated the start, stop and abnormal operations of the IFMIF without the beam. The second group calculations simulated the normal operations of the IFMIF with the beam. In both groups, the calculations were performed through two steps as follows. In the first step, thermal calculations of the steady state heat transfer option were performed to obtain various temperature distributions using different thermal boundary conditions. In the second step, structural calculations of the linear static option were performed,

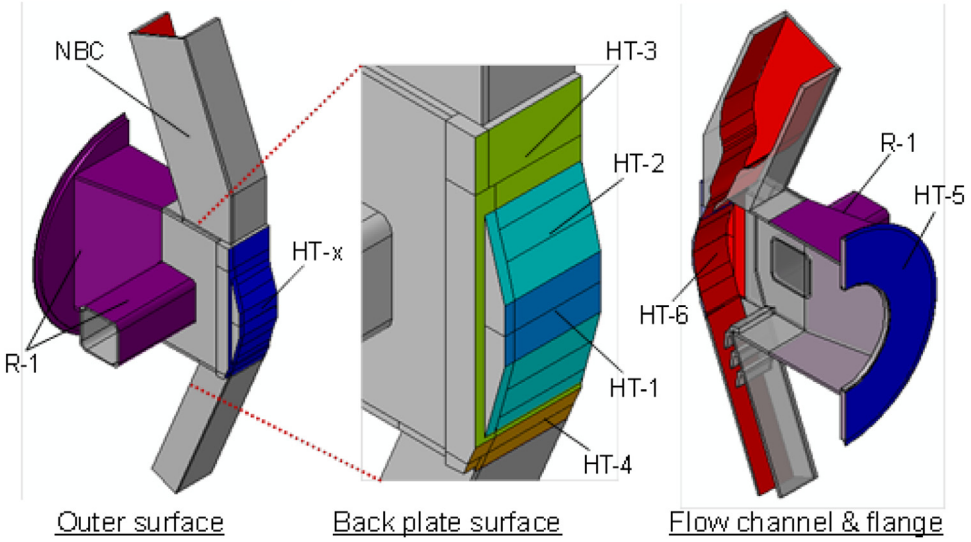

Fig. 5. Classification of the thermal boundary conditions in the outer surface, back plate surface, and flow channel and flange.

Table 2
List of calculation cases (*) a room temperature (No Li in flow channels).

Case ID	Group	Step	Temperature of boundary simulating Li (˚C)	Heating simulating nuclear heat
Case-T11	1. Simulating	(1) Thermal	300	Off
Case-T12	IFMIF start/		250	
Case-T13	stop or		200	
Case-S11	abnormal	(2) Structural	20*→250→300	
Case-S12	operations		300→250→20*	
Case-S13			300→250→200→20*	
Case-T21	2. Simulating	(1) Thermal	300	On
Case-S21	IFMIF	(2) Structural	300	Off→On
Case-S22	normal operations		300	On→Off

based on the temperature distributions obtained in the first step. The calculation cases of two groups are listed in Table 2. In thermal calculations of step 1, the boundary conditions were set. In this section, heater model was replaced by heat transfer from liquid Li. The thermal boundary conditions are listed in Table 3. In the structural calculations of step 2, the constraint conditions for the displacement and rotation were set. The calculated temperature of the lithium flow channel was estimated higher than 200 ˚C. While in the other part of the target assembly, for example the flange, the body and the support, the calculated temperature was estimated lower than 200 ˚C. Because the melting point of lithium is about 180 ˚C, the lithium flow channel shall be preheated above 190 ˚C including a margin.

Table 4
Summary of calculated results (*) occurred in body.

Case ID	*Max. von Mises stress (MPa)*		Magnitude	*Maximum displacement (mm)*		
	in TA	in BP		X	Y	Z
Case-S11	117.2*	60.3	2.875	− 1.369	1.173	2.831
Case-S12	371.9*	364.1	0.724	0.350	− 0.248	− 0.700
Case-S13	281.9*	272.8	1.165	− 0.566	− 0.423	− 1.149
Case-S21	8.43	8.43	3.14E−3	− 3.12E−3	1.92E−3	− 9.49E−4
Case-S22	8.44	8.44	3.12E−3	3.12E−3	− 1.92E-3	9.49E−4

4. Calculation results of target assembly

The calculation results are summarized in Tables 4 and 5. In Fig. 6, temperature distribution of target assembly (TA) with heater control. The calculated deformation results of Case-S11 and Case-S21in the target assembly and the back plate are shown in Fig. 7, where the deformations are exaggerated by factors of 50 for the target assembly, 200 for the back plate, respectively. This analysis was done to estimate integrity of the integrated TA under the design pressure and the design temperature before Li charge.

4.1. Transition process and normal keeping temperature condition

To compare the results in Case-S11 and in Case-S12, it was not a reversible process for the temperature ascent and the temperature descent. (The temperature distribution was changed from uniform to non-uniform in Case-S11, while it was changed from non-uniform to

Table 3
List of thermal boundary conditions.

Marks in Fig. 5	Models	Locations	Heat transfer coefficient (W/m^{2}K)	Emissivity (-)	Boundary Temp. (˚C)
HT-1	Heat transfer	BP / HFTM	43.4	–	50
HT-2		BP / HFTM	11.0	–	50
HT-3		Frame / HFTM	7.81	–	50
HT-4		Frame / HFTM	6.72	–	50
HT-5		Flange / Flange	15.8	–	50
HT-6		Flow channel / Li	3.4E4	–	200 ~ 300
R-1	Radiation	Outer (far from Li)	–	0.3	50
NBC	No (Adiabatic)	Outer (near to Li)	–	–	–

Table 5
Power density in each region (W/mm^3).

X-div.	Y-div.	Z-div.						
		A	B	C	D	E	F	G
Layer 3	6	2.242e−3	2.057e−3	1.909e−3	1.597e−3	1.189e−3	8.887e−4	5.549e−4
	5	3.826e−3	3.460e−3	3.116e−3	2.629e−3	1.987e−3	1.383e−3	6.694e−4
	4						1.724e−3	7.919e−4
	3						1.964e−3	8.881e−4
	2						2.228e−3	1.002e−3
	1						2.365e−3	1.047e−3
Layer 2	6	2.516e-3	2.254e-3	2.070e−3	1.686e−3	1.199e−3	8.314e−4	5.155e−4
	5	4.424e-3	3.956e-3	3.628e−3	2.798e−3	1.924e−3	1.099e−3	6.221e−4
	4					2.448e−3	1.301e−3	7.224e−4
	3					2.895e−3	1.520e−3	8.416e−4
	2					3.374e−3	1.704e−3	9.314e−4
	1					3.636e−3	1.868e−3	1.021e−3
Layer 1	6	2.516e−3	2.254e−3	2.070e−3	1.686e−3	1.199e−3	8.314e−4	5.155e−4
	5	4.981e−3	4.299e−3	3.670e−3	2.568e−3	1.592e−3	1.043e−3	6.221e−4
	4	1.023e−2	7.667e−3	5.634e−3	3.546e−3	2.016e−3	1.219e−3	7.224e−4
	3	2.247e−2	1.494e−2	8.608e−3	4.516e−3	2.472e−3	1.440e−3	8.416e−4
	2	2.488e−2	1.661e−2	1.003e−2	5.273e−3	2.832e−3	1.660e−3	9.314e−4
	1	2.599e−2	1.754e−2	1.089e−2	5.852e−3	3.158e−3	1.843e−3	1.021e−3

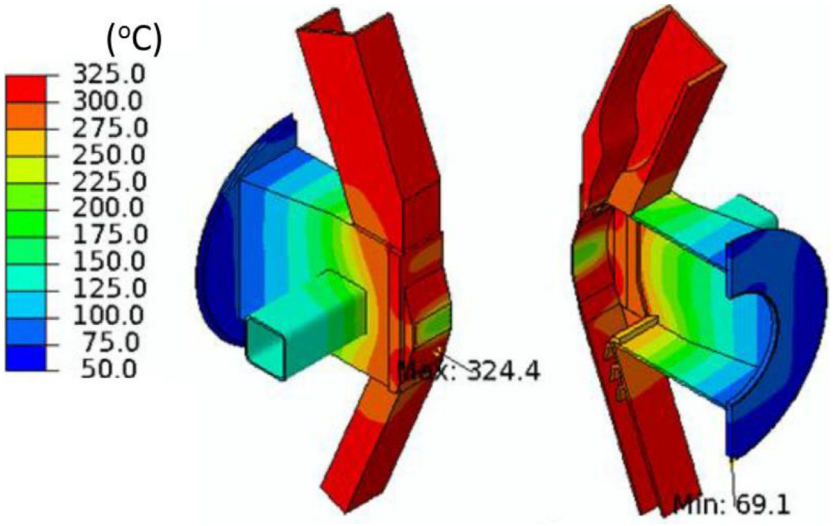

Fig. 6. Temperature distribution of target assembly (TA) (before Li charge).

uniform in Case-S12.) The maximum value of von Mises stress in Case-S12 was more than three times as large as that in Case-S11. The maximum displacement was observed in Case-S11, and it was to be 2.875 mm in the instantaneous elevated temperature process from RT to 250 °C in the operation preparation process under a condition of no nuclear heating and no lithium flowing, and the magnitude of deformation can be reduced by the decrease of the elevating temperature rate.

In Case-S13, to add a step of 200 °C into the temperature descent process, the maximum stress was equal to 3/4 in Case-S12. The calculated maximum von Mises stress, 282 MPa was lower than the permissible stress of F82H, 423 MPa which was defined by the yield stress at 300 °C. The maximum Mises stress was found to be 372 MPa in transient cooling process from 300 °C. In actual phenomenon, it is expected that the temperature changing progress more slowly, so the thermal stress will be reduced furthermore. Therefore a soundness of the target assembly could be estimated. To compare the results in Case-S21 and in Case-S22, it was a reversible process for the beam on and the beam off. In both cases, the maximum von Mises stresses and magnitude displacements were nearly same each other, and the maximum displacements in each direction had the same values and reverse directions each other. In those cases to change thermal conditions of the beam on and off, the calculated stresses and displacements were small enough, so it was considered that there was no problem for thermal soundness of the target assembly. In this case, it was possible to estimate the temperature range of the lithium flow channel, 200 °C to 325 °C by adjusting the input data of the heat flux of the heaters. The maximum temperature of the TA is 325 °C, and it is still lower than the Li boiling point of 344 °C under a vacuum pressure of 10^{-3} Pa. The TA temperature was reduced and became uniform, almost equaled to Li temperature (250 °C typically) after starting of Li circulation through the TA with heater control at the same time.

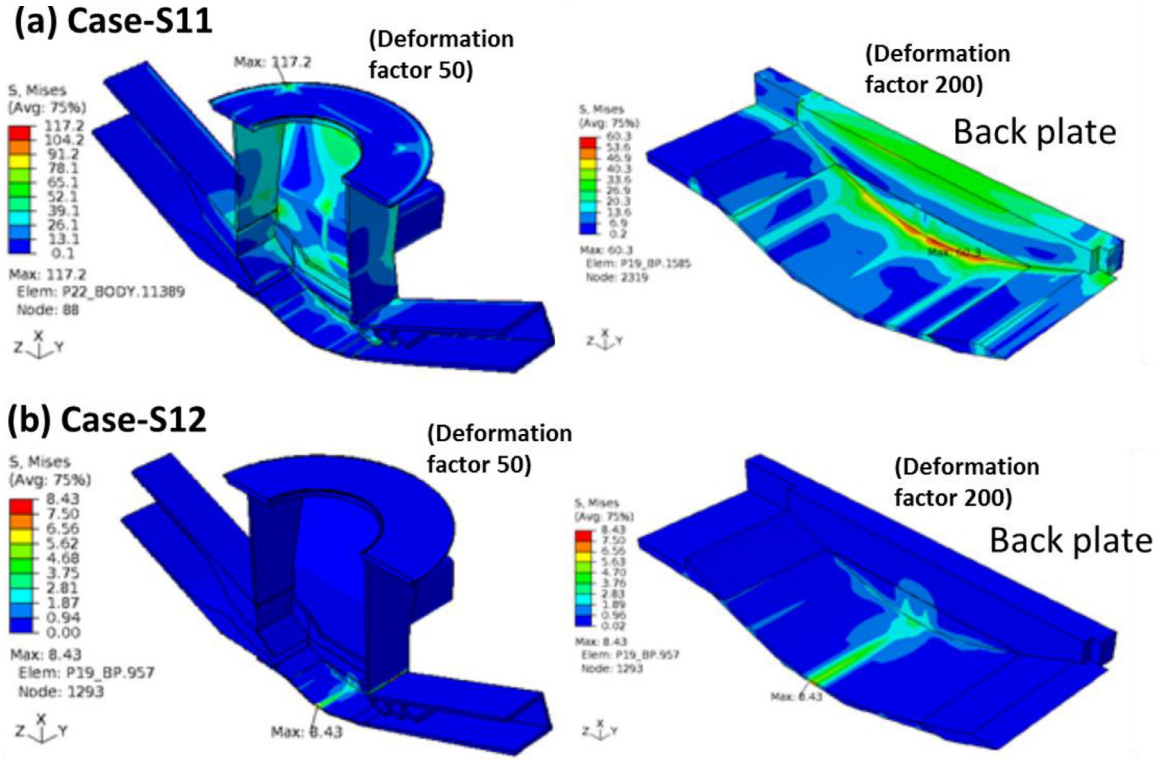

Fig. 7. Calculated deformation results (a) Case-S11 and (b) Case-S21in the target assembly and the back plate.

4.2. Nuclear heating caused by neutron flux

On the IFMIF normal operations, there will be the beam with 250 mA of 40 MeV deuterons which has its footprint with 200 mm in width and 50 mm in height on the back plate center. The input data of the nuclear heating were based on those due to neutron through Li and secondary gamma through Li, based on the calculation of Simakov et al. [31,32]. The neutrons are produced in the exothermic ^{7}Li(d, n)^{8}Be reaction. The yield of these high energy neutrons is relatively small (0.5%), but they have significant importance for the nuclear heating, activation and shielding behavior. The input data of the nuclear heating were based on those due to neutron through Li and secondary gamma through Li. In the gamma-ray yield produced in the Li target. There are two physical processes which produce photons in the lithium target: first, the primary reaction Li(d, xγ), and, second, neutron induced secondary reactions such as the inelastic scattering of source neutrons on lithium nuclei, i.e. the Li(n, xγ) reaction. Both of these production paths were analysed by means of McDeLicious calculations using the evaluated INPE data for d + ^{6,7}Li and n + ^{6,7}Li. The contribution of the neutron induced gamma-ray production depends on the size and mass of the lithium target. For the Li target, it amounts to about 8% of the deuteron induced gamma-ray yield, which, in turn, is one order of magnitude less than the total neutron yield.

In this study, to simulate the power distribution of the nuclear heating, calculation model of the back plate was divided into sub-regions three-dimensionally. In thermal calculation with the beam of group 2, the nuclear heating was loaded as the power density as shown in Table 5, and the distributions of nuclear heating in back plate of the target assembly is evaluated and is shown in Fig. 8.

5. Conclusion

In the IFMIF operation, intense neutrons are emitted inside the Li flow through a thin back plate attached to the target assembly. Since the back plate is operating under a severe neutron irradiation of 50 dpa/year and a maximum nuclear heating rate of 25 W/cm^3, thermo-structural design is one of critical issues in a target design. The back plate is replaced in annual maintenance after every 11 months operation because of neutron irradiation damage. In this study the engineering design of a target assembly of IFMIF lithium target was performed in IFMIF/EVEDA project for a high intensity neutron source. The “integrated type” target assembly versus the target assembly model with replaceable bayonet-type back plate were evaluated. Thermos-structural analysis of the target assembly was evaluated by ABAQUS code. The applied material for the target assembly including the back plate was F82H steel. In the thermal-structural analysis, the normal operations and start/stop or abnormal operations were evaluated in the temperature condition at 250 or 300 °C operation of Li flow in the inlet pipe of the target assembly. The result in all conditions were showed that the temperature of the target assembly was evaluated to be still lower than the Li boiling point of 344 °C under a vacuum pressure of 10^{-3} Pa. In a temperature constant operation, the calculated stresses and displacements were small enough for thermal soundness of the target assembly in steady states. In a transient cooling process from 300 °C to 20 °C through 250 °C, the maximum Mises stress was found to be 372 MPa, which was lower than the yield stress at 300 °C.

Conflict of interest

This research paper was the result of “The design and thermo-structural analysis of target assembly for high intensity neutron source”

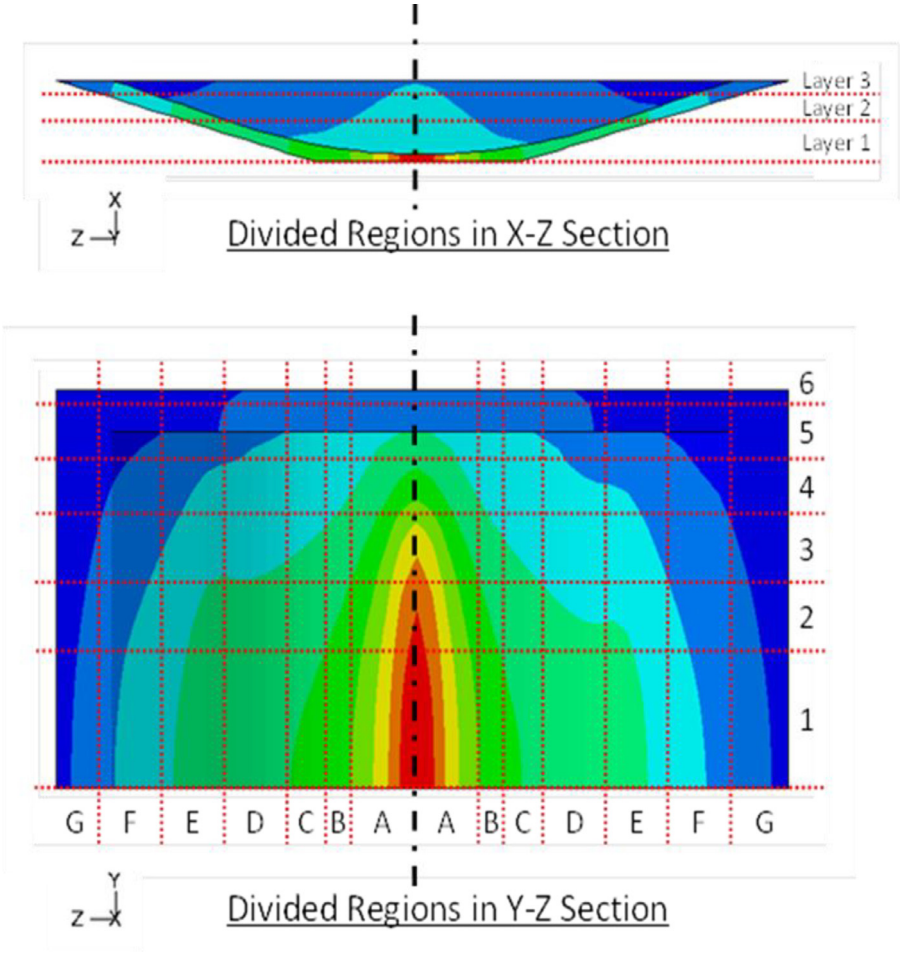

Fig. 8. Distributions of nuclear heating in back plate of the Li target assembly. *X* axis is the vertical direction of *YZ* plane which is basically the intermediate of two beam directions, *Y* axis is the horizontal direction, and *Z* axis is the perpendicular direction.

entrusted to Japan Atomic Energy Agency performed under IFMIF/EVEDA project.

Acknowledgments

The activity was performed under the IFMIF/EVEDA project. The authors are grateful to the members of IFMIF/EVEDA EU and JA members, fusion for energy and related ones. Especially, we would like to express appreciation to Dr. R. Heidinger of F4E, Drs. G. Micciche, D. Bernardi, and S. Nitti of ENEA, Drs. F. Arbeiter, K. Tian, V. Heinzel, and A. Moselang, A. Ibarra of CIEMAT in EU team, and Drs. M. Ida, K. Nakamura, S. Niitsuma, H. Nakamura, K. Fujishiro, T. Kanemura, T. Nishitani, M. Sugimoto, H. Kimura, S. Ohira, Profs. E. Hoashi, S. Yoshihashi-Suzuki, H. Horiike, Y. Tsuji, T. Terai, S. Fukada, J. Yagi, A. Suzuki,and Ms. M. Hirano of JA team, and Drs. P. Garin, H. Matsumoto, J. Knaster, K. Fujishiro, and M. Perez of IFMIF/EVEDA project team, Profs. T. Muroga, T. Yokomine, and A. Kohyama for their fruitful discussion and coordination.

References

[1] E. Wakai, T. Kanemura, H. Kondo, Y. Hirakawa, Y. Ito, H. Serizawa, Y. Kawahito, T. Higashi, A. Suzuki, S. Fukada, K. Furuya, K. Esaki, J. Yagi, Y. Tsuji, T. Ito, S. Niitsuma, S. Yoshihashi-Suzuki, K. Watanabe, T. Furukawa, F. Groeschel, G. Micciche, S. Manorri, P. Favuzza, F.S. Nitti, R. Heidinger, T. Terai, H. Horiike, M. Sugimoto, S. Ohira, J. Knaster, Engineering validation for lithium target facility of the IFMIF under IFMIF/EVEDA project, Nuclear Mater. Energy 9 (2016) 278–285.

[2] E. Wakai, H. Kondo, T. Kanemura, T. Furukawa, Y. Hirakawa, K. Watanabe, M. Ida, Y. Ito, S. Niitsma, Y. Edao, K. Fujishiro, K. Nakaniwa, E. Hoashi, H. Horiike, H. Serizawa, Y. Kawahito, S. Fukada, Y. Sugie, A. Susuki, J. Yagi, Y. Tsuji, K. Furuya, F. Groeschel, J. Knaster, G. Micchiche, A. Ibarra, R. Heidinger, F. Nitti, M. Sugimoto, Engineering validation and engineering design of lithium target facility in IFMIF/EVEDA project, Fus. Sci. Technol. 66 (2014) 46–56.

[3] E. Wakai, H. Kondo, M. Sugimoto, S. Fukada, J. Yagi, M. Ida, T. Kanemura, T. Furukawa, Y. Hirakawa, K. Fujishiro, A. Suzuki, T. Terai, Y. Edao, T. Hiromoto, S. Shigeharu, S. Niitsuma, H. Kimura, H. Horiike, E. Hoashi, S. Suzuki, N. Yamaoka, H. Serizawa, Y. Kawahito, Y. Tsuji, K. Furuya, F. Takeo, Development of Lithium Target System in Engineering Validation and Engineering Design Activity of the International Fusion Materials Irradiation Facility (IFMIF/EVEDA), J. Plasma Fus. Res. 88 (2012) 691–705.

[4] J. Knaster, P. Garin, H. Matsumoto, Y. Okumura, M. Sugimoto, F. Arbeiter, P. Cara, S. Chel, A. Facco, P. Favuzza, T. Furukawa, R. Heidinger, A. Ibarra, T. Kanemura, A. Kasugai, H. Kondo, V. Massaut, J. Molla, G. Micciche, S. O'hira, K. Sakamoto, T. Yokomine, E. WakaiIFMIF/EVEDA Integrated Project Team, Overview of the IFMIF/EVEDA project, Nucl. Fus. 57 (2017) 102016(25pp).

[5] L. Mansur, Materials research and development for the spallation neutron source mercury target, J. Nucl. Mater 318 (2003) 14–25.

[6] H. Takada, K. Haga, M. Teshigawara, T. Aso, S. Meigo, H. Kogawa, T. Naoe, T. Wakui, M. Ooi, M. Harada, M. Futakawa, Materials and Life Science Experimental Facility at the Japan Proton Accelerator Research Complex I: Pulsed Spallation Neutron Source, Quantum Beam Sci. 1 (2017) 2017, 8-pp.1–26.

[7] J.R. Haines, T.J. McManamy, T.A. Gabriel, R.E. Battle, K.K. Chipley, J.A. Crabtree, L.L. Jacobs, D.C. Lousteau, M.J. Rennich, B.W. Riemer, Spallation neutronsourcetargetstationdesign, development, and commissioning, Nuclear Instrum. Methods Phys. Res. A 764 (2014) 94–115.

[8] Y. Dai, G.S. Bauer, Status of the first SINQ irradiation experiment, STIP-I, J. Nucl. Mater 296 (2001) 43–53.

[9] L.K. Mansur, J.R. Haines, Status of the Spallation Neutron Source with focus on target materials, J. Nucl. Mater 356 (2006) 1–15.

[10] T. McManamy, M. Rennich, F. Gallmeier, P. Ferguson, J. Janney, 3MW solid rotating target design, J. Nucl. Mater 398 (2010) 35–42.

[11] A.R. Paramo, F. Sordo, J.M. Perlado, A. Rivera, Viability of the ESS-Bilbao neutron source for irradiation of nuclear fusion materials, J. Nucl. Mater 444 (2014) 469–474.

[12] X.J. Jia, G.S. Bauer, W. He, Y.L. Sun, T.J. Liang, W. Yin, D. Zha, Mock-up stands for

a rotating target for CSNS project, J. Nucl. Mater 398 (2010) 28–34.
[13] F.S. Nitti, A. Ibarra, M. Ida, P. Favuzza, T. Furukawa, F. Groeschel, R. Heidinger, T. Kanemura, J. Knaster, H. Kondo, G. Micchiche, M. Sugimoto, E. Wakai, The design status of the liquid lithium target facility of IFMIF at theend of the engineering design activities, Fus. Eng. Des 100 (2015) 425–430.
[14] F. Arbeiter, N. Baluc, P. Favuzza, F. Groeschel, R. Heidinger, A. Ibarra, J. Knater, T. Kanemura, H. Kondo, V. Massaut, F.S. Nitti, G. Micchiche, S. O'hira, D. Rapisarda, M. Sugimoto, E. Wakai, T. Yokomine, The accomplishments of lithium target and test facility validation activities in the IFMIF/EVEDA phase, Nucl. Fus. 58 (6pp) (2018) 015001.
[15] H. Kondo, T. Kanemura, T. Furukawam Y. Hirakawa, E. Wakai, Cavitation inception upstream of liquid lithium target for intense fusion neutron source, Fus. Eng. Des. 124 (2017) 990–994.
[16] T. Kanemura, H. Kondo, T. Furukawa, Y. Hirakawa, E. Hoashi, S. Yoshihashi, H. Horiike, E. Wakai, Measurement of Surface Velocity of Li Target in IFMIF/EVEDA Li Test Loop, Fus. Eng. Des. 109-111 (2016) 1682–1686.
[17] H. Kondo, T. Kanemura, T. Furukawa, Y. Hirakawa, E. Wakai, J. Knaster, Experimental Study on Cavitation of a Liquid Lithium Jet for International Fusion Materials Irradiation Facility, J. Nuclear Eng. Radiat. Sci. 3 (2017) 041005-1 – 041005-11.
[18] H. Kondo, T. Kanemura, T. Furukawa, Y. Hirakawa, E. Wakai, J. Knaster, Validation of liquid lithium target stability for an intense neutron source, Nucl. Fus. 57 (2017) 066008.
[19] P. Favuzza, A. Antonelli, T. Furukawa, F. Groeschel, R. Heidinger, T. Higashi, Y. Hirakawa, M. Iijima, Y. Ito, T. Kanemura, J. Knaster, H. Kondo, G. Micciche, F.S. Nitti, S. Ohira, M. Severi, M. Sugimoto, A. Suzuki, R. Traversi, E. Wakai, Round robin test for the determination of nitrogen concentration in solid lithium, Fus. Eng. Des. 107 (2016) 13–24.
[20] E. Wakai, et al., Nitrogen hot trap design and manufactures for lithium test loop in IFMIF/EVEDA project, Plasma Fusion and Res. 11 (2016) 2405112-1 to 4.
[21] H. Nakamura, P. Agostini, K. Ara, S. Fukada, K. Furuya, P. Garin, et al., Latest design of liquid lithium target in IFMIF, Fus. Eng. Des. 84 (2009) 252–258.
[22] K. Watanabe, M. Ida, H. Kondo, N. Nakamura, E. Wakai, Thermo-structural analysis of integrated back plate in IFMIF/EVEDA liquid lithium target, Fus. Eng. Des. 86 (2011) 2482–2486.
[23] J. Knaster, F. Arbeiter, P. Cara, S. Chel, A. Facco, R. Heidinger, A. Ibarra, A. Kasugai, H. Kondo, G. Micciche, K. Ochiai, S. O'hira, Y. Okumura, K. Sakamoto, E. Wakai, IFMIF, the European–Japanese efforts under the Broader Approach agreement towards a Li(d,xn) neutron source: Current status and future options, Nuclear Mater. Energy 9 (2016) 46–54.
[24] M. Ida, H. Kondo, K. Nakamura, E. Wakai, Hydraulic analysis on effects of backplate deformation upon stability of high-speed free-surface lithium flow for IFMIF target design, Fus. Eng. Des. 86 (2011) 2478–2481.
[25] K. Esaki, K. Hiyane, S. Fukada, E. Wakai, Y. Ito, F. Nitti, Study on control of nonmetallic impurities in liquid lithium, J. Plasma Fus. Res. SERIES 11 (2015) 36–40.
[26] S. Yoshihashi-Suzuki, E. Hoashi, T. Kanemura, H. Kondo, N. Yamaoka, H. Hiriike, Characteristics of surface oscillation on high speed liquid Li jet, Fus. Eng. Des. **87**, 2012, 1434–1438.
[27] E. Hoashi, S. Yoshihashi-Suzuki, H. Nanba, T. Kanemura, H. Kondo, T. Furukawa, N. Yamaoka, H. Horiike, Numerical study on free surface flow of liquid metal lithium for IFMIF, Fus. Eng. Des. 88 (2013) 2515–2519.
[28] J. Yagi, A. Suzuki, T. Terai, Nitrogen contamination effect on yttrium gettering of hydrogen in liquid lithium, J. Nucl. Mater 417 (2011) 710–712.
[29] M. Ida, H. Nakamura, H. Nakamura, H. Nakamura, K. Ezato, H. Takeuchi, Thermal-hydraulic characteristics of IFMIF liquid lithium target, Fus. Eng. Des. 63–64 (2002) 333.
[30] T. Yokomine, T. Yoshida, T. Kunugi, E. Wakai, Neutronic Analysis of IFMIF High Flux Test Module for High Temperature Irradiation, Fus. Sci. Technol. 68 (2015) 657–661.
[31] S.P. Simakov, U. Fischer, U. von Moellendorff, I. Schmuck, A. Konobeev, P. Pereslavtsev, Advanced Monte Carlo procedure for the IFMIF d-Li neutron source term based on evaluated cross section data, J. Nucl. Mater 307–311 (2002) 1710–1714.
[32] S.P. Simakov, U. Fischer, K. Kondo, P. Pereslavtsev, Status of the McDeLicious Approach for the D-Li Neutron Source Term Modeling in IFMIF Neutronics Calculations, Fus. Sci. Technol. 62 (2012) 233–239.